1236 *Biochemistry* **2010,** *49,* 1236–1247
DOI: 10.1021/bi9020617

BIOCHEMISTRY
including biophysical chemistry & molecular biology
Article

Biochemical Characterization of Native Usher Protein Complexes from a Vesicular Subfraction of Tracheal Epithelial Cells[†]

Marisa Zallocchi,[‡] Joseph H. Sisson,[§] and Dominic Cosgrove*[,‡]

[‡]*Usher Syndrome Center, Boys Town National Research Hospital, 555 North 30th Street, Omaha, Nebraska 68131, and* [§]*University of Nebraska Medical Center, Omaha, Nebraska 68198*

Received August 5, 2009; Revised Manuscript Received January 4, 2010

ABSTRACT: Usher syndrome is the major cause of deaf/blindness in the world. It is a genetic heterogeneous disorder, with nine genes already identified as causative for the disease. We noted expression of all known Usher proteins in bovine tracheal epithelial cells and exploited this system for large-scale biochemical analysis of Usher protein complexes. The dissected epithelia were homogenized in nondetergent buffer and sedimented on sucrose gradients. At least two complexes were evident after the first gradient: one formed by specific isoforms of CDH23, PCDH15, and VLGR-1 and a different one at the top of the gradient that included all of the Usher proteins and rab5, a transport vesicle marker. TEM analysis of these top fractions found them enriched in 100−200 nm vesicles, confirming a vesicular association of the Usher complex(es). Immunoisolation of these vesicles confirmed some of the associations already predicted and identified novel interactions. When the vesicles are lysed in the presence of phenylbutyrate, most of the Usher proteins cosediment into the gradient at a sedimentation coefficient of approximately 50 S, correlating with a predicted molecular mass of 2×10^6 Da. Although it is still unclear whether there is only one complex or several independent complexes that are trafficked within distinct vesicular pools, this work shows for the first time that native Usher protein complexes occur *in vivo*. This complex(es) is present primarily in transport vesicles at the apical pole of tracheal epithelial cells, predicting that Usher proteins may be directionally transported as complexes in hair cells and photoreceptors.

Usher syndrome (USH)[1] is defined by congenital, bilateral deafness and a later onset of visual loss caused by *Retinitis pigmentosa* (RP) in humans. It is the most common form of combined deaf/blindness with a prevalence of approximately one person in 25000. Vestibular dysfunction is also a clinical feature of specific USH subtypes (*1*−*3*). This genetically heterogeneous disorder can be divided in three clinical subtypes, namely, USH1, USH2, and USH3. USH type 1 is the most severe form of the disease. USH1 patients are deaf at birth, the onset of RP is prepubertal, and most of them have vestibular dysfunction. USH2 is characterized by a moderate to severe hearing loss at birth, and RP can be diagnosed during puberty. USH3 has a later initiation of deafness combined with variable RP and vestibular dysfunction. Usher syndrome can also be associated with reduced odor identification, impaired sperm motility, and mental deficiency (reviewed in refs *4* and *5*).

Of the 11 loci responsible for this syndrome, 9 have been already identified (*6*−*17*). Misense mutations in 4 of the USH1 genes (B, C, D, and F) are also associated with nonsyndromic hearing loss, suggesting that specific isoforms are important for inner ear function but not retina (*18*, *19*).

The Usher proteins belong to protein classes with very distinct functions (*5*, *18*, *19*). Myosin 7A (USH1B) is an unconventional myosin motor protein found associated with actin microfilaments in the stereocilia, in the hair cell body, and in the neuroretina (*20*). Harmonin (USH1C), SANS (USH1G), and whirlin (USH2D) are scaffold proteins (*15*, *21*−*26*), and cadherin 23 (CDH23, USH1D) and protocadherin 15 (PCDH15, USH1F) are members of the cadherin superfamily of Ca^{2+}-dependent cell adhesion molecules (*27*−*30*). In the case of USH2A, the short form of usherin (isoform a) is an extracellular matrix protein (*31*−*34*) while the long isoform (isoform b) is a transmembrane protein. VLGR-1b (USH2C) belongs to the G-protein coupled receptor superfamily with a unique ectodomain consisting of seven calcium exchange β repeats that may play a role in cell−cell adhesion (*35*). Finally, clarin-1, the USH3A gene product, is a transmembrane protein that belongs to the tetraspanin family, with a possible role in synaptic remodeling (*36*, *37*).

With the exception of SANS, all of the Usher proteins are expressed as multiple isoforms that can be regulated in a tissue-specific and/or developmental manner. Examples of these are the isoform b of harmonin that is exclusively expressed in the inner

[†]Supported by NIH Grants R01 DC004844 to D.C. and 5R37AA008769-17 to J.H.S.

*Address correspondence to this author. Phone: (402) 498-6334. Fax: (402) 498-6331. E-mail: cosgrove@boystown.org.

[1]Abbreviations: ANK, ankyrin; BSA, bovine serum albumin; CC, coiled coil; CDH23, cadherin 23; cen, central; C-t, C-terminal; CT, cytoplasmic; EC, extracellular cadherin; EGF-Lam, laminin-type EGF-like; FCS, fetal calf serum; FN3, fibronectin type III; GST, glutathione *S*-transferase; LamG, laminin G; LamGL, laminin G-like; LamNT, N-terminal laminin; LN, laminin globular-like domain; mRNPs, messenger ribonucleoprotein particles; nm, nanometers; NRS, normal rabbit serum; OCT, optimal cutting temperature; PBA, phenylbutyric acid; PBS, phosphate-buffered saline; PBM, PDZ-binding motif; PCHD15, protocadherin 15; PDZ, postsynaptic protein PSD-95/SAP90, *Drosophila* septate junction protein Discs-large, and tight junction protein ZO-1 homology domain; PST, serine- and threonine-rich sequence; PVDF, polyvinylidene fluoride; RBC, red blood cells; RP, *Retinitis pigmentosa*; SAM, sterile alpha motif; TEM, transmission electron microscopy; TG, thyroglobulin; TM, transmembrane; USH, Usher syndrome; USH1, USH type 1; UHS2, USH type 2; USH3, USH type 3; VLGR-1, very large G-protein coupled receptor 1.

 Published on Web 01/08/2010

ear (*38*), CDH23-containing exon 68, which is only expressed at the tip of the stereocilia (*39*), and clarin-1 that is transiently expressed at the afferent synaptic terminals that innervate outer hair cells during cochlea synaptogenesis (*37*).

There is increasing evidence suggesting the existence of functional Usher complexes *in vivo* in hair cells and photoreceptors, with a central role for the PDZ domain containing protein homologues, harmonin and whirlin (reviewed in ref *19*). In most of the cases these two proteins bind to either C-terminal class I PDZ-binding motifs or to internal PDZ-binding domains present in their corresponding partners (*11*, *21*, *40*−*45*). All of the other USH1 proteins (myosin 7A, CDH23, SANS, and PCDH15) and the USH2 proteins (usherin b and VLGR-1b) have been described to interact with harmonin and whirlin. Moreover, it has been suggested that the Usher complex is associated to the cytoskeleton network through harmonin, directly, via the PST domain present in isoform b or indirectly via its interaction with myosin 7A.

In addition to these interactions, many of the Usher proteins (myosin 7A, harmonin, whirlin, SANS, CDH23, and PCDH15) form homodimers, incorporating an extra degree of complexity to the Usher network (reviewed in refs *5*, *45*−*47*).

With the exception of the interaction between CDH23 and PCDH15, which has been demonstrated *in vivo* at the tip of the hair cells (*48*), all evidence suggesting the presence of an Usher complex is based on colocalization studies, GST-pull down assays, and/or coimmunoprecipitation experiments using specific domains of the Usher proteins overexpressed in heterologous cell systems (*11*, *21*, *29*, *42*, *44*, *49*). Studies demonstrating native Usher protein interactions are lacking, probably due to the low abundance of cochlear hair cells and photoreceptors, which precludes analysis using common biochemical techniques.

On the basis of previous studies showing expression of myosin 7A (USH1B) and whirlin (USH2D) in a variety of ciliated cells and bovine tissues (*25*, *49*), combined with the knowledge that all of the Usher proteins are localized in ciliated sensory neuroepithelia (hair cells in inner ear and photoreceptors in retina), we hypothesized that tracheal epithelial cells might provide a good model for examining native Usher protein interactions *in vivo*.

Using bovine trachea as a source of Usher proteins and sucrose density gradients, we show that all of the proteins cosediment in a buoyant subfraction enriched in rab5 positive vesicles. When these vesicles are lysed in the presence of a chemical chaperone and layered in a second sucrose density gradient, most of the Usher proteins cosediment in the middle of the gradient with a sedimentation coefficient of approximately 50 S units. Whether there is more than one independent Usher complex trafficked in the same or distinct vesicular pools remains unresolved. Coimmunoprecipitation of these vesicles with specific antibodies against different Usher proteins confirms not only the vesicular nature of the Usher complex but also some of the interactions involved in its formation, providing direct evidence for the existence of native Usher protein interactions *in vivo*.

EXPERIMENTAL PROCEDURES

Antibody Generation. Fusion peptide constructs comprising the first coiled-coil domain of harmonin (amino acids 319−409), part of the transmembrane and cytoplasmic domains of CDH23 (amino acids 2950−3170), the cytoplasmic domain of PCDH15-CD1 (*30*) (amino acids 1483−1703), amino acids 200−400 of SANS, and the C-terminal region of usherin b (usherin C-t), were constructed using the FLAG-ATS expression system (Sigma, St. Louis, MO). The recombinant proteins were expressed in *Escherichia coli* and purified from supernatant following osmotic shock and using a nickel affinity chromatography, according to the methods provided by the manufacturer. Antibodies were raised in rabbits under contract with Chemicon (Temecula, CA) and affinity purified according to methods previously described by Bhattacharya et al. (*32*). The antibody preparations were qualified by immunofluorescence of mouse retinas, using the peptide antigen as a competitive inhibitor. Acetone-fixed tissue was incubated in 10% milk blocking solution with the antibody alone or in the presence of a 100-fold molar excess of the corresponding fusion peptide as described (*37*).

Other Antibodies. The mouse monoclonal myosin 7A antibody and the rabbit polyclonal antibodies against the C-terminal VLGR-1 (VLGR-1 C-t, amino acids 6159−6306), the LN domain of usherin, and clarin-1 have already been described (*32*, *37*, *50*, *51*). The rabbit anti-CDH23(−68) antibody specific to the cytoplasmic domain was generously provided by Dr. U. Muller (*27*, *39*).

Commercially available antibodies are goat anti-harmonin (NB100−1405; Novus Biologicals, Littleton, CO), goat anti-whirlin (S-19), and goat anti-ribosomal protein S6 (E-13) (sc-49787 and sc-13007, respectively; Santa Cruz Biotechnology, Santa Cruz, CA), mouse monoclonal antiacetylated tubulin and anti-rab5 (T6793 clone 6-11B-1 and R7904 clone Rab5-65, respectively; Sigma, St. Louis, MO), rat polyclonal anti-Na^+/K^+ ATPase, beta 1 subunit (06-170; Upstate Biotechnology, NY), Alexa Fluor 488 donkey anti-rabbit and Alexa Fluor 555 goat anti-mouse (Molecular Probes-Invitrogen, Eugene, OR), anti-goat IgG, anti-rabbit IgG, anti-mouse IgG, and anti-rat IgG-peroxidase conjugated antibodies (Sigma, St. Louis, MO).

Animals. Wild-type mice were in the 129 Sv/J strain, obtained from Jackson Laboratories (Bar Harbor, ME) and bred in-house. All of the experiments using mice were carried out under an approved IACUC protocol, and every effort was made to minimize pain and discomfort related to experimental use of mice. Bovine tracheas were provided by contract from a local meat packing facility (Nebraska Beef Co., Omaha, NE).

Isolation of Mouse Tracheal Epithelial Cells. Five-week-old mice were used for tracheal epithelial cell isolation. Briefly, the perfused trachea was microdissected and the inner ciliated epithelia scraped in PBS containing 0.1 mM ATP. Cells were mechanically dissociated in the presence of EDTA (0.2%), and red blood cells (RBC) were removed by incubation of the pelleted cells with ammonium chloride solution (20 mM Tris, 100 mM NH_4Cl, pH 7.2) for 5 min at 4 °C. The dissociated RBC-free cells were fixed with 50 μL of 4% paraformaldehyde containing 30% sucrose for 30 min at room temperature. Five microliters of the cell suspension was applied to each slide and allowed to dry at room temperature. The attached cells were used for immunofluorescence studies.

Immunofluorescence. Bovine trachea rings were fixed with 4% paraformaldehyde in 0.1 M phosphate buffer (pH 7.4), paraffin-embedded, and sectioned at 8 μm thickness.

Mouse trachea rings were fixed with 1% paraformaldehyde in 0.1 M phosphate buffer (pH 7.4) containing sucrose (30%) for 2 h at 4 °C, mounted in OCT, frozen, and cryosectioned at 14 μm thickness.

Sections or isolated mouse tracheal epithelial cells were incubated in a blocking/permeabilizing solution for at least

30 min at room temperature (PBS, 0.1% Triton X-100, and 5% FCS) and then incubated overnight in the same blocking solution with the corresponding primary antibody. After three washes with PBS, the sections were incubated for 1 h at room temperature in blocking solution with a 1:600 dilution of the appropriate secondary IgG Alexa-conjugated antibody. The dilutions for the primary antibodies were as follows: 1/300 dilution for rabbit harmonin, CDH23, PCDH15, VLGR-1 C-t, and clarin-1; 1/500 dilution for SANS and usherin C-t, 5 μg/mL for acetylated tubulin, and 2 μg/mL for rab5.

Slides were coverslipped using Vectashield mounting medium (Vector, Burlingeme, CA) and images captured using a Zeiss Axio Imager A1 or a Zeiss AxioPlan 2IF MOT microscope interfaced with a LSM510 META confocal imaging system. Final figures were assembled using Adobe Photoshop and Illustrator software (Adobe System, San Jose, CA).

Electron Microscopy. The isolation and preparation of the vesicles for transmission electron microscopy were as described by Deretic and Papermaster (*52*). Briefly, the buoyant fractions from the first sucrose gradient (11, 12, and 13, where the Usher proteins were found) were diluted with 1 volume of 10 mM Tris-HCl, pH 7.4, containing 1 mM $MgCl_2$ and protease inhibitors, and centrifuged at 28000 rpm for 1 h in a SW28 Beckman Coulter centrifuge. The pelleted vesicles were fixed with 3% glutaraldehyde in Sørensen buffer containing 7.5% sucrose. The fixed vesicles were mixed with 2% cooled low melting point agarose and processed for electron microscopy.

Usher Complex Isolation. One fresh bovine trachea (30 cm in length) was collected biweekly and used as a regular source of Usher proteins. The luminal epithelia were dissected from the trachea and homogenized in buffer containing 10 mM Tris−Ac, pH 7.4, 0.25 M sucrose, 1 mM $MgCl_2$, and protease inhibitors (40 μM bestatin B8385, 20 μM antipain A6191, 0.8 μM aprotinin A1153, 1 μg/mL pepstatin P5318, and 100 μM leupeptin L2884; Sigma, St. Louis, MO). The homogenate was cleared by centrifugation, and the Usher complexes were isolated as described by Papermaster and Dreyer (*53*) and Deretic and Papermaster (*52*) for the isolation of rhodopsin from postgolgi membranes, with some modifications. Briefly, the homogenates were layered in a continuous 20−39% sucrose gradient with a 49% sucrose cushion and centrifuged for 20 h at 22000 rpm using a SW28 swinging bucket rotor (Beckman Coulter). Fourteen fractions were collected from the bottom to the top of the gradient and analyzed by Western blot.

The top fractions presenting detectable Usher proteins were pooled and diluted with 1 volume of homogenization buffer without sucrose containing protease inhibitors and 10 mM 4-phenylbutyric acid (PBA; Sigma, St. Louis, MO). The vesicles were disrupted by the addition of Triton X-100 (2 mg of detergent/mg of protein), layered in a 10−40% second sucrose gradient, and sedimented at 24000 rpm for 16 h. Fractions were collected as before and analyzed by Western blot.

Polyacrylamide gels loaded with the same volumes as for the Western blots were run in parallel and silver stained (Bio-Rad, 161-0449).

Coimmunoprecipitation Studies. The vesicle-containing Usher proteins were concentrated (see Electron Microscopy section) and immunoprecipitated as described before (*52*). Briefly, the concentrated vesicles were resuspended in a small volume of the same buffer and mixed with 40 μL of a 50% slurry suspension of protein A−Sepharose beads (P3391; Sigma, St. Louis, MO) that were precoated with normal rabbit IgG or with 1 μg of the specific rabbit antibodies against the following Usher proteins: VLGR-1 C-terminus, usherin C-terminus, harmonin, and SANS. The incubations were conducted for 2 h at 4 °C with constant rocking. After several washes the immunoprecipitates were resuspended in sample buffer and analyzed by Western blot.

Western Blot. The 14 samples from the first and second sucrose gradients were incubated with sample buffer in the presence of reducing agents for 40 min at 55 °C and then resolved in SDS−PAGE, transferred to PVDF membrane overnight using 35 V at 4 °C, and blocked overnight at 4 °C in 10% nonfat dry milk containing 0.2% Tween 20. The incubation with the primary antibody was done in blocking solution overnight at 4 °C. The dilutions used for each antibody were as follows: 1/2500 for anti-myosin 7A; 3 μg/mL for anti-harmonin, anti-CDH23, and anti-VLGR-1; 2 μg/mL for anti-PCDH15, anti-SANS, and anti-clarin-1; 1/500 dilution for anti-whirlin and anti-LN domain of usherin (usherin C-t was not used for immunoblotting as it did not react with the denatured form of bovine usherin); 1/1000 dilution for anti-Na^+/K^+ ATPase beta 1 subunit and anti-rab5. After two washes the membranes were incubated with the secondary antibodies for 1 h in blocking solution (anti-rabbit HRP-conjugated antibody 1/20000, anti-mouse, anti-rat, and anti-goat HRP-conjugated antibodies 1/1000) at room temperature. After four additional washes the specific protein bands were revealed using the ECL system (Pierce 32209) or SuperSignal West Femto system (Pierce 34094) in the case of rab5 immunoblots and usherin second sucrose gradient . Membranes were also incubated with preimmune rabbit serum as a control for specificity of the Usher antibodies developed in our laboratory.

The immunoprecipitates were boiled for 5 min in the presence of sample buffer with reducing agents, and the proteins were resolved in a SDS−PAGE and transferred to PVDF membranes for 1 h using 100 V at 4 °C. Incubations with anti-CDH23, anti-PCDH15, and anti-LN domain of usherin were done as described above. Membranes were also immunoblotted with goat anti-harmonin 1/500 and rabbit anti-CDH23(−68) 1/1000.

Biochemical Estimation of the Usher Complex's Molecular Mass. (*A*) *Bovine Serum Albumin* (*BSA*) *and Thyroglobulin Standards*. BSA fraction V (03117332001; Roche Diagnostics, Indianapolis, IN) and thyroglobulin (T1001; Sigma, St. Louis, MO) were layered in a 10−40% sucrose density gradient and run in parallel with the second sucrose gradient of the vesicular fraction. Again, 14 samples were collected from the bottom to the top of the gradient, but in this case the fractions containing the protein standards were detected by Coomassie Blue staining of polyacrylamide gels.

(*B*) *Ribosomal Preparation*. The large and small ribosomal subunits were obtained as described by Napoli et al. (*54*) with few modifications. Briefly, total mouse brain was homogenized in ribosomal buffer (100 mM NaCl, 10 mM $MgCl_2$, 10 mM Tris-HCl, pH 7.5, 1 mM dithiothreitol, 30 units/mL Invitrogen RNase OUT, 1% Triton X-100, and 10 μL/mL Sigma protease inhibitor cocktail P8340), incubated 5 min on ice, and centrifuged at 10000*g* for 10 min at 4 °C. The cleared supernatant was layered in a 10−40% sucrose gradient and run in parallel with the second sucrose gradient containing vesicles. Fractions were analyzed by absorbance at 260 nm. A sample of each fraction was also assayed for the presence of the ribosomal protein S6 (a marker for the small ribosomal subunit) by Western blot 1/500 dilution.

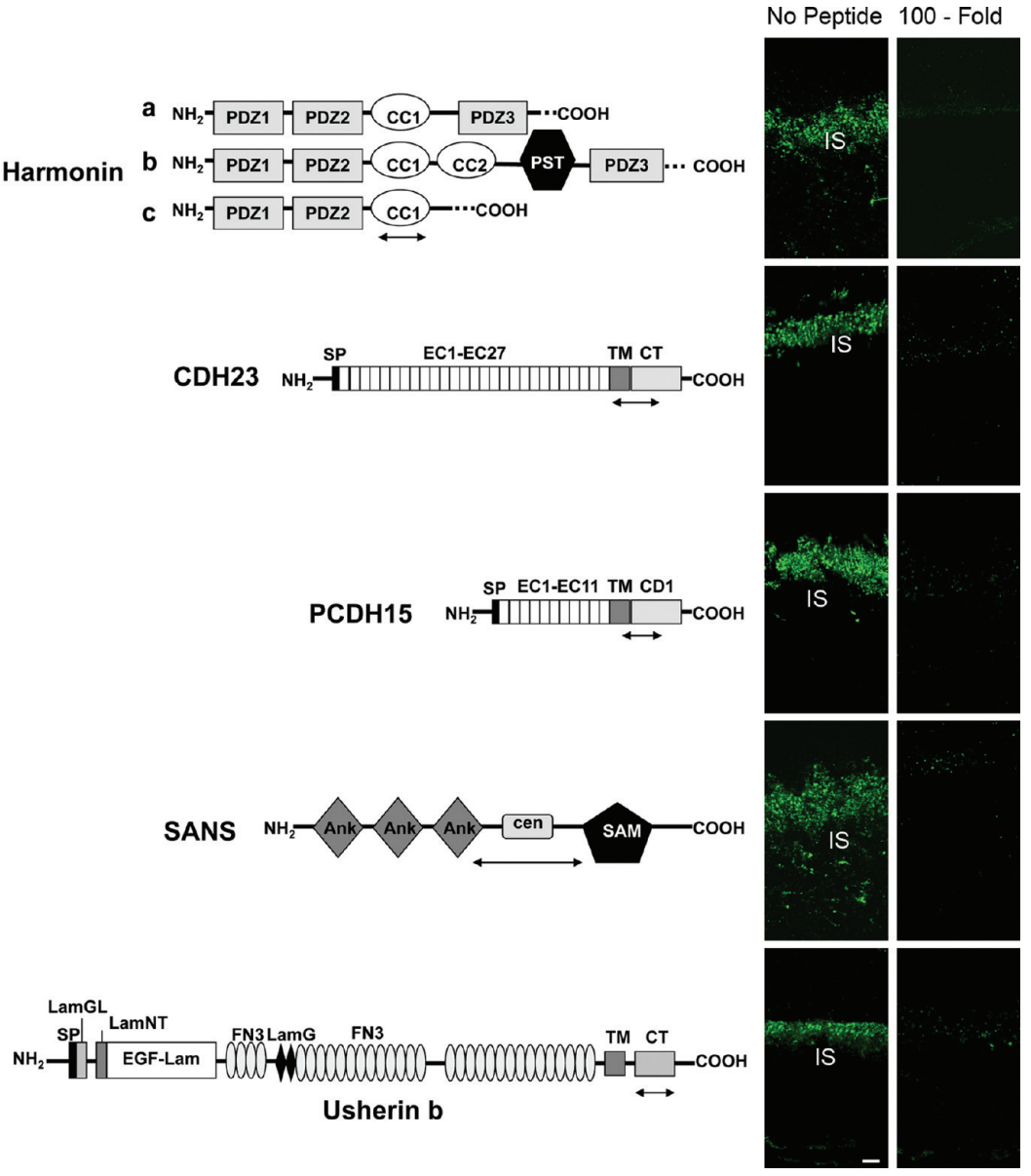

FIGURE 1: Anti-Usher antibody qualification. Left: Predicted structures of the different Usher syndrome related proteins with the immunogenic regions for the antibodies produced indicated as a double arrow. There are three classes of harmonin isoforms. Harmonins a and b have three PDZ domains while harmonin c has only two. Harmonins a and c have one coiled-coil (CC) domain. Harmonin b has an extra coiled-coil domain and a serine- and threonine- (PST) rich sequence. Cadherin 23 and protocadherin 15 contain several extracellular cadherin (EC) repeats and a transmembrane (TM) and a cytoplasmic (CT) domain. Multiple splice variants have been identified for both cadherins. SANS has three ankyrin- (ANK-) like motifs, a central domain (cen) followed by a sterile alpha motif (SAM), and a PDZ-binding motif (PBM) at the C-terminus. Usherin b contains a laminin G-like domain (LamGL), an N-terminal laminin domain (LamNT), 10 laminin-type EGF-like modules (EGF-Lam), 32 fibronectin type III (FN3) repeats spaced by two laminin G domains (LamG) followed by a TM domain, and a CT domain containing a PBM. Right: Confocal microscopy of postnatal day 28 mouse retinas incubated with the indicated anti-Usher antibody alone (no peptide) or in the presence of a 100-fold molar excess of the fusion peptide used to generate it (100-fold). IS: inner segment. Scale bar: 5 μm.

RESULTS

Antibody Specificity. To test the specificity of the antibodies developed by our laboratory, we used a tissue for which the expression of the Usher proteins has already been well characterized (*5*, *19*, *29*, *45*). Postnatal day 28 mouse retinas were immunostained with the specific rabbit anti-Usher protein antibodies alone or in the presence of a 100-fold molar excess of the immunogen used to generate the antibody (Figure 1). As shown by others (*5*, *19*, *29*, *45*) there is strong immunostaining in the inner segments (IS) of photoreceptor cells for all five Usher antibodies. The signal disappears in the presence of an excess of the fusion peptide, demonstrating the specificity of these antibodies. Mouse retina immunostained with preimmune rabbit IgG was negative (data not shown).

Detection of the Usher Proteins in Bovine and Mouse Tracheal Epithelia Cells. Bovine trachea rings were used for immunohistochemistry to analyze the expression and localization of the Usher proteins. Figure 2 (panels A−G) shows that all of the Usher proteins are present in the ciliated epithelia of bovine trachea, with the most robust immunostaining consistently observed near the ciliary axonemes (arrowheads). Given the limitations of working with bovine tissue in terms of morphology preservation and the fact that we could not find a good ciliary marker for bovine ciliated epithelia, we also analyzed the subcellular localization of the Usher proteins in

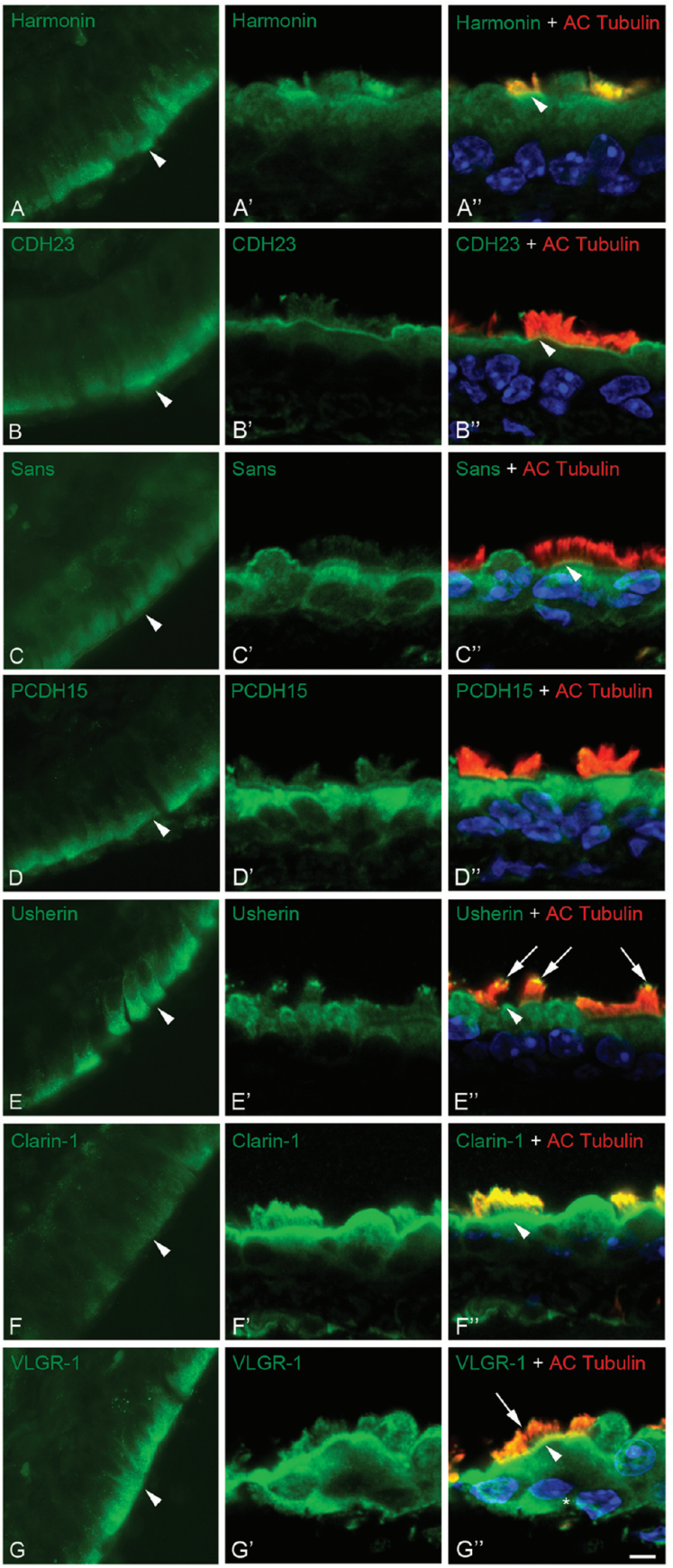

FIGURE 2: Expression of the Usher proteins in bovine and mouse trachea. A−G: Immunofluorescence analysis of paraffin-embedded sections of bovine tracheal rings. Magnification: 200×. A′−G′ and A″−G″: Dual confocal immunostaining of mouse tracheal rings with the different Usher antibodies (green) and acetylated tubulin (red), a marker for the cilia axoneme. DAPI was used for nuclear counterstaining (blue). Arrowheads denote the basal body region and arrows the immunostaining for usherin and VLGR-1 at the tip of the cilia. Scale bar: 3 μm.

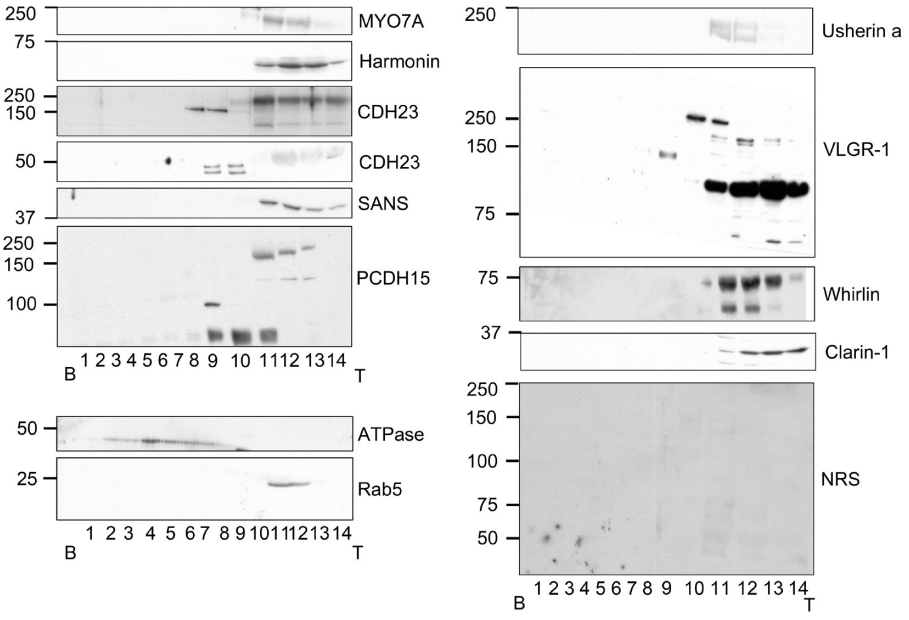

FIGURE 3: Western blot analysis of Usher proteins following sucrose gradient fractionation. Most of the Usher protein isoforms were found near the top of the gradient (fractions 11−13). Specific isoforms of cadherin 23, protocadherin 15, and VLGR-1 sedimented further into the gradient. The fractions were also assessed for the presence of the Na^+/K^+ ATPase, beta 1 subunit, and rab5. Molecular weight markers are indicated. B: bottom of the gradient. T: top of the gradient. Results represent one of at least four independent experiments.

mouse trachea by dual immunostaining with acetylated tubulin, a marker for the cilia axoneme (Figure 2, panels A′−G′ and A″−G″). Similar to the expression in bovine trachea, all of the Usher proteins are present at the base of the cilia (arrowheads). Harmonin, usherin, clarin-1, and VLGR-1 are also expressed at the cilia, with harmonin and clarin-1 present all along the cilia (shown by colocalization with acetylated tubulin) and usherin and VLGR-1 only present at the tip (arrows). Myosin 7A and whirlin are also expressed in trachea (refs *25* and *49* and data not shown).

Study of the Usher Protein Interactions and Their Association with Vesicles. Bovine tracheal epithelium was homogenized and cleared and then fractionated by sucrose density gradient (20−39%), and fractions were analyzed by Western blot for all of the Usher proteins. Figure 3 shows an example of these results in which all of the Usher proteins cosedimented between fractions 11 and 13 (the buoyant fraction): Myosin 7A (200 kDa), harmonin (70 kDa), SANS (45 kDa), and clarin-1 (30 kDa) are present as single bands with molecular masses that are similar to the ones already reported for other species (see refs *5*, *18*, and *19* for reviews). Two different isoforms of CDH23 (250 and 120 kDa) are detected in the same fractions, likely corresponding to isoforms a and b, respectively (*55*). There are three bands for PCDH15 (250, 130, and 90 kDa) representing three different isoforms of PCHD15-CD1 (*30*). The LN-domain antibody developed against usherin detects a double band at 200 kDa corresponding to the short isoform (isoform a). VLGR-1 shows one prominent band at around 100 kDa, another at 170 kDa (probably isoform a), and an undescribed isoform at 250 kDa. Finally, of the five isoforms already described for whirlin (*25*) we only detect two (75 and 50 kDa).

A distinct group of isoforms for CDH23, PCDH15, and VLGR-1 sediments between fractions 8 and 10, suggesting the possible existence of a cytosolic complex between these three proteins. Anti-CDH23 antibodies detect a 150 kDa band and a doublet at 50 kDa, corresponding to isoforms b/d and c_{1-2}, respectively. PCDH15 Western blots show two bands at 110 kDa and the one at 90 kDa, and VLGR-1 shows a single band at 140 kDa.

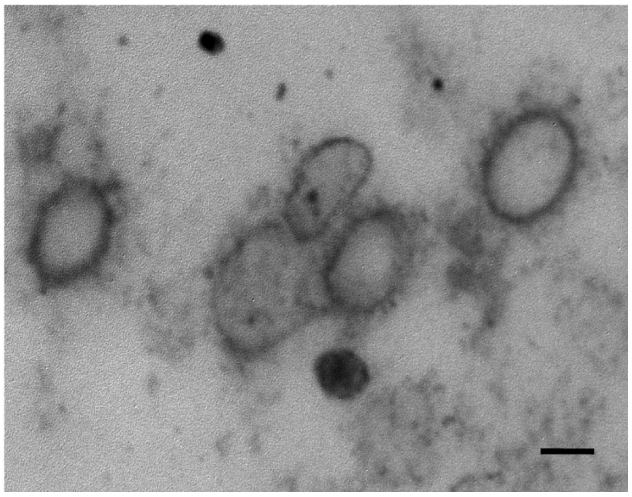

FIGURE 4: Electron microscopy confirmation of vesicles in the top fractions of the first sucrose gradient. TEM image shows that the pooled fractions (11−13) are rich in 100−200 nm vesicles, consistent in size with transport vesicles. Bar: 100 nm.

The unrelated plasma membrane protein Na^+/K^+ ATPase sediments differently in the gradient, demonstrating that plasma membrane fragments are not present in the buoyant fraction of our preparations, and thus the Usher proteins, which are in the buoyant fractions, are either present as monomers or as vesicular complexes.

Rab5, a vesicular protein involved in docking of the vesicles to the plasma membrane (*56*) sediments in the same fractions (11−13) as all of the Usher proteins. We focused our studies on fractions 11−13 because we expected the Usher proteins were forming complexes, and their position at the top of the gradient, coordinate with the vesicle-associated protein rab5, could thus be explained by their association with vesicles.

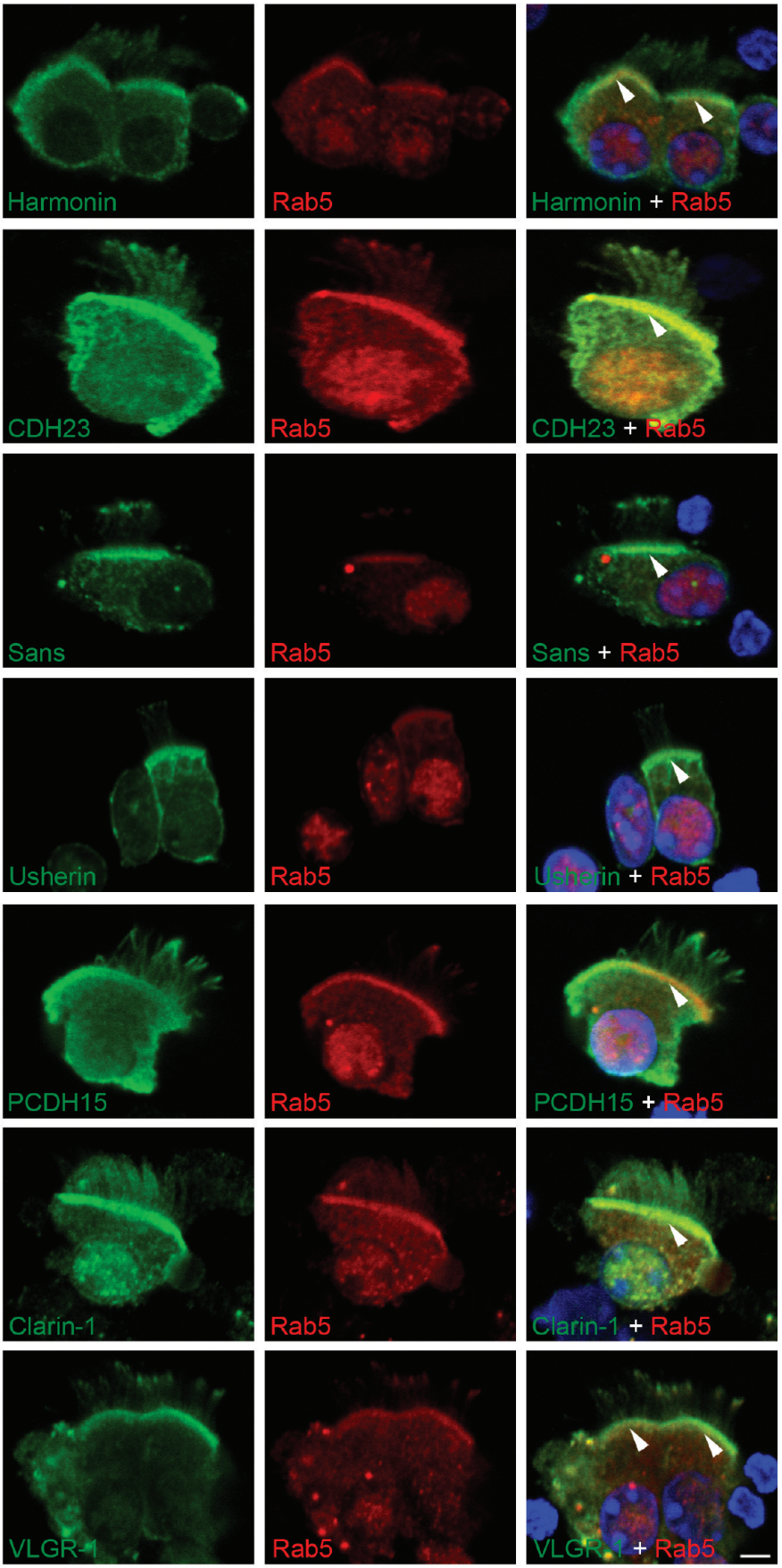

FIGURE 5: Colocalization studies between the Usher proteins and the vesicular marker rab5. Isolated mouse tracheal epithelial cells were double stained with anti-Usher protein antibodies (green) and anti-rab5 antibodies (red). DAPI was used for nuclear counterstaining (blue). Arrowheads denote the transition zone/basal body area where all of the Usher antibodies show colocalization with rab5. Scale bar: 3 μm.

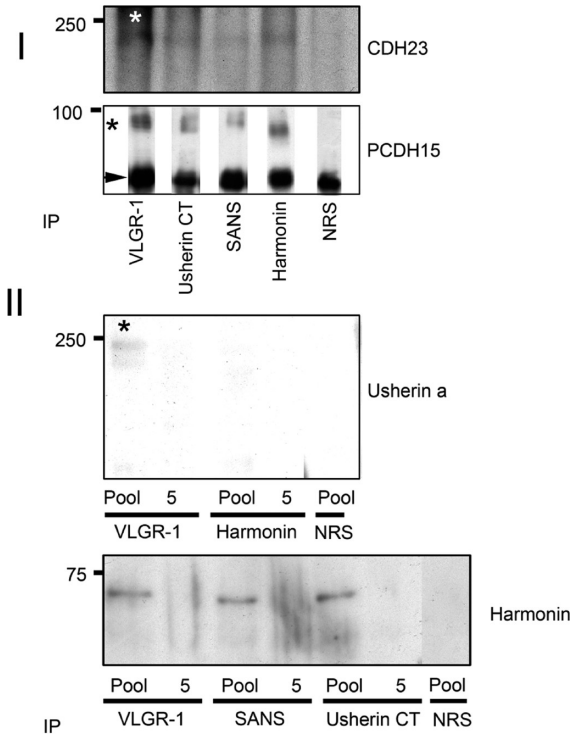

FIGURE 6: Coimmunoprecipitation of Usher proteins from the vesicular fraction. Panel I: The concentrated vesicles were immunoprecipitated with specific anti-Usher antibodies and probed with anti-CDH23(−68) (top) or anti-PCDH15-CD1 (bottom) antibodies. Panel II: The pooled vesicles or fraction 5 was immunoprecipitated and probed with anti-usherin (top) or goat anti-harmonin (bottom) antibodies. Results represent an example of three independent experiments. Asterisks denote specific coimmunoprecipitated proteins. The arrowhead in panel 1 denotes IgG heavy chain cross-reactivity. Pool = IP of pooled fractions 11−13; 5 = IP of fraction 5 (negative control, since fraction 5 contains no Usher proteins); NRS = preimmune rabbit IgG.

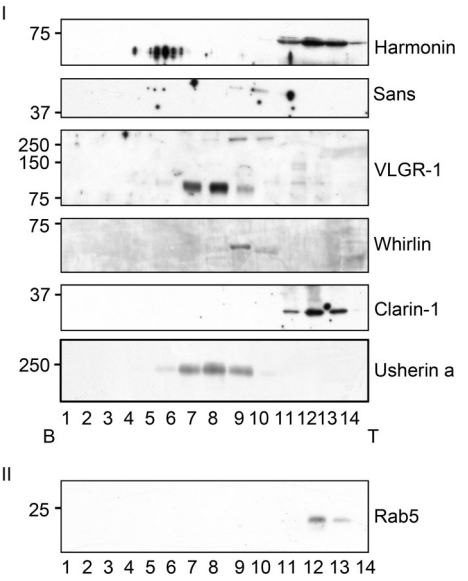

FIGURE 7: Western blot analysis of the Usher proteins following lyses of the vesicles and resedimentation on a second sucrose gradient. Panel I shows that SANS, VLGR-1, whirlin, and usherin sedimented in the middle of the gradient, while harmonin, clarin-1, and the vesicle marker rab5 (panel II) remained at the top of the gradient. B: bottom of the gradient. T: top of the gradient. Results represent an example of at least three independent experiments.

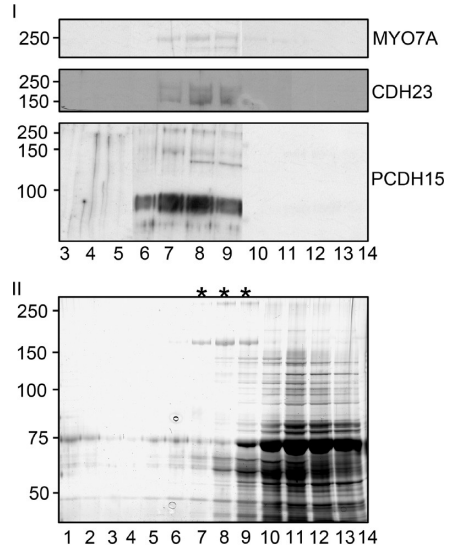

FIGURE 8: Western blot analysis of the Usher proteins following lyses of the vesicles and resedimentation on a second sucrose gradient. Panel I: Myosin 7A, CDH23, and PCDH15 sedimented in the middle of the gradient. Panel II: Silver-stained PAGE showing the total protein present in the fractions from the second sucrose gradient. Asterisks at the top denote lanes representing the fractions where Usher proteins were detected on Western blots. Results represent an example of at least three independent experiments.

To determine directly whether vesicles are present at the top of the gradient, fractions 11, 12, and 13 were pooled, concentrated, and processed for transmission electron microscopy. Results shown in Figure 4 demonstrate indeed that these fractions are enriched in 100−200 nm vesicles, consistent in size to transport vesicles.

Results from Figures 3 and 4 strongly suggest that one or more Usher complexes are been trafficked in transport vesicles in the tracheal epithelia.

Dual immunostaining of isolated tracheal epithelial cells with antibodies specific for the different Usher proteins and rab5 (Figure 5) suggests the Usher proteins may be present in rab5-positive vesicles, since they all show overlapping staining with rab5. There is intense dual immunostaining at the base of the cilia (arrowheads) suggesting an accumulation of the Usher proteins and rab5 at the transition zone/basal body area. There is also staining, although varying in localization and intensity, in the ciliary axoneme for all of the Usher proteins.

To assess directly the existence of a complex(es) of Usher proteins, the concentrated vesicles were subjected to immunoprecipitation with specific rabbit antibodies against some of the Usher proteins. Protein interactions could be demonstrated by immunoprecipitation using antibodies specific for usherin C-t, VLGR-1, SANS, and harmonin. Rabbit preimmune serum was used as a control for specificity. The results in Figure 6 (panel I) show that VLGR-1, usherin b, SANS, and harmonin interact with isoform "a" of CDH23 (250 kDa) and the 90 kDa isoform of PCHD15-CD1. Both anti-CDH23 antibodies, the one developed in our laboratory and the anti-CDH23(−68), recognize the same isoform of CDH23 by coimmunoprecipitation. Only the immunoblot with anti-CDH23(−68) is shown. Harmonin complexes with VLGR-1, SANS, and usherin b (Figure 6, panel II bottom) are present in the vesicular fraction but not with usherin a. However, there is an interaction between VLGR-1 and usherin a (Figure 6, panel II top). Absence of these bands when immunoprecipitations are performed using normal rabbit serum or a

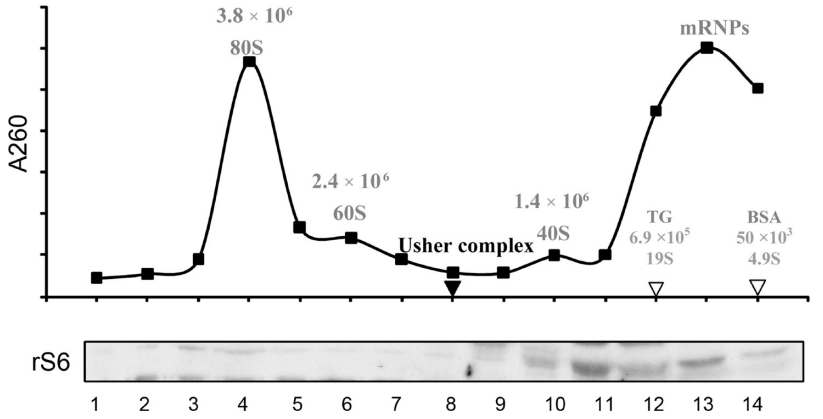

FIGURE 9: Estimation of the size of the Usher protein complex(es). Top: Ribosomes were fractionated on a 10−40% sucrose gradient. The intact 80S monosome, the 60S and 40S ribosomal subunits, and the mRNPs were detected by absorbance at 260 nm. Position and molecular weights (*60*) are indicated. We included peak fractions and sedimentation coefficient values for thyroglobulin (TG) (*61*), bovine serum albumin (BSA), and the Usher complex. Bottom: Immunodetection of the small ribosomal protein subunit S6 (rS6) from each ribosomal fraction by Western blot. The Usher complexes peak at fractions 8 and 10.

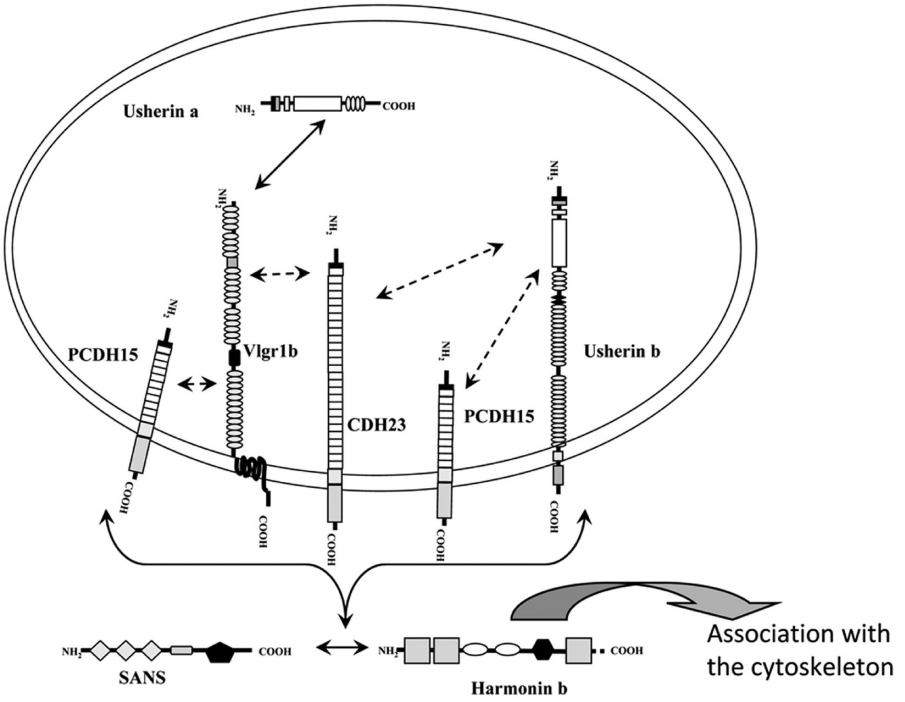

FIGURE 10: Schematic representation of the interactions between the Usher proteins. The interactions between VLGR-1, usherin, PCDH15, CDH23, harmonin, and SANS are shown within the vesicle context. Double arrows indicate interactions that occur between specific domains or with a specific orientation: Harmonin and SANS (present outside the vesicles) interact with the cytoplasmic domains of VLGR-1, usherin b, PCDH15, and CDH23. The interaction between harmonin and SANS occurs at the cytoplasmic face of the vesicles. The interaction between VLGR-1 and usherin occurs in the lumen of the vesicles. Double dashed arrows indicate interactions that take place between the Usher proteins, but the specific domains or the specific orientation was not established: VLGR-1 and usherin b interact with PCDH15 and CDH23. These interactions can occur inside the vesicle or facing the cytosol. Harmonin connects the whole vesicular complex with the cytoskeleton network directly through its PST domain or indirectly via its interaction with myosin 7A.

different fraction from the first sucrose gradient (labeled "5") confirms the specificity of the coimmunoprecipitation experiments.

Estimation of the Size of the Usher Complex. To determine approximately the size of the Usher complex, the vesicles in the pooled fractions were lysed in the presence of phenylbutyric acid (PBA) and then fractionated in a second 10−40% continuous sucrose density gradient. PBA is a chemical chaperone that helps to maintain hydrophobic interactions between molecules due to its amphiphatic properties (*57*, *58*). Figures 7 and 8 show that when the vesicles are lysed, VLGR-1, usherin a isoform, myosin 7A, CDH23, and PCDH15 sediment well into the gradient mostly between fractions 7 and 9, suggesting that they may participate in the formation of a macromolecular Usher protein complex. A second smaller potential Usher protein complex comprised of SANS, whirlin, and a 250 kDa isoform of VLGR1 sediments to fractions 9 and 10. Only harmonin and clarin-1 remain at the top (Figure 7), suggesting that under these conditions they are not present in an Usher protein complex(es). Figure 6 shows that harmonin coimmunoprecipitates with VLGR1, SANS, and usherin b, implying that harmonin is indeed forming complexes with several Usher proteins; however, these interactions apparently dissociate under the conditions used for the second sucrose gradients. Upon vesicle disruption rab5

remains in the top fractions, demonstrating that it is not part of a large protein complex.

The 14 fractions were also resolved in a SDS−PAGE and silver stained to gain an appreciation of the complexity of the proteins present in these fractions. The results shown in Figure 8 (panel II) demonstrate that these fractions (fractions 7, 8, and 9) do indeed contain a large number of proteins, but most at a low abundance. It is notable that these are the only fractions that contain very high molecular mass proteins (some of them larger than 250 kDa).

Thyroglobulin, BSA, and a brain ribosomal preparation were fractionated on 10−40% sucrose gradients in parallel as sedimentation coefficient standards to estimate the size of the Usher complex(es). Figure 9 shows the positions of intact 80S ribosome (peaks at fraction 4) and the two ribosomal subunits, 60S (peaks at fraction 6) and 40S (peaks at fraction 10), as well as the very light messenger ribonucleoprotein particles (mRNPs). The positions of thyroglobulin (19S) and BSA (4.9S) are also indicated. Western blots for the small ribosomal protein S6 (part of the 40S ribosomal subunit) were run in parallel to independently confirm the fractions containing 80S intact ribosomes and the 40S ribosomal subunits. The Usher protein complex(es) (black arrowhead) sediments between the 60S (MW 2.4×10^6) and the 40S subunits (MW 1.4×10^6). While sucrose gradients are not entirely linear with respect to molecular mass of complexes, we expect the complex to be around 50S with a molecular mass of the larger Usher protein complex of approximately 2×10^6 Da. The smaller complex would be close to the size of the 40S ribosomal subunit (about 1.4×10^6 Da). These data confirm that these proteins are sedimenting as a macromolecular complex(es) and, in combination with the findings presented in Figure 6, strongly support the existence of native Usher protein complex formation in tracheal epithelial cells.

DISCUSSION

Earlier work suggesting Usher proteins interact to form complexes is based on colocalization studies in hair cells and photoreceptors and on interactions between specific domains of the different Usher proteins overexpressed as fusion peptides in heterologous cell lines (*29*, *42*, *44*, *47*, *49*, *59*). Our study provides evidence for native Usher protein interactions.

Deretic and Papermaster (*52*) demonstrated that it is possible to isolate transport vesicles by continuous sucrose density gradients. Using the same approach we were able to discriminate between two different classes of possible Usher protein complexes. The first was found in the top fractions of the gradients colocalizing with rab5-positive transport vesicles. Although we suggest one Usher complex in the buoyant fraction, we cannot rule out the possibility of more than one independent Usher complex, packed in the same or distinct transport vesicle subpools, with some of the proteins (i.e., harmonin) present in more than one complex.

The second Usher complex detected after the first sucrose gradient is smaller and appears to be cytosolic (i.e., not vesicle associated), involving the association of specific isoforms of CDH23, PCDH15, and VLGR-1.

Coimmunoprecipitation studies using the concentrated vesicles from the buoyant fraction allowed us not only to confirm the *in vivo* relevance of some of the Usher protein interactions (*29*, *45*) but also to establish new ones (see Figure 10 for a schematic representation). The coimmunoprecipitation of PCDH15, CDH23, and harmonin with antibodies that recognized the cytoplasmic domains of VLGR-1 and usherin b implies a cytosolic localization for these domains in the vesicular context, with their ectodomains facing the lumen of the vesicles. Harmonin and SANS face the cytosol where they interact with VLGR-1 and usherin b through their cytoplasmic domains. Harmonin associates with usherin b but not usherin a, which lacks the PDZ-binding motif that was previously shown to interact with harmonin by GST pull-down assays (*21*, *24*, *29*, *44*).

We show a novel interaction between usherin a and VLGR-1, which likely involves cell matrix binding motifs, and would thus be predicted to occur in the vesicular lumen (Figure 10). It has already been shown that usherin a is a basement membrane component that associates specifically to type IV collagen and fibronectin in retinal basement membranes (*33*, *34*) and also to heterodimeric transmembrane receptors like integrins (unpublished data). The fact that VLGR-1 is the only Usher protein that is also located at the basal aspect of the tracheal ciliated epithelia where usherin a is expressed (*31*) suggests a biological relevance of this interaction at the basal aspect of the ciliated epithelia.

We speculate that the Usher proteins are associated with the transition zone/basal body area and possibly involved in the docking of proteins destined for transport into the cilia and/or the regulation of cilia motility.

One of the limitations of our approach is the amount of manipulations needed to concentrate the vesicle fraction for coimmunoprecipitation. It is possible that some of the Usher protein associations are unstable and dissociate during the procedure. We also might be disrupting some of the secondary and all the tertiary/quaternary associations, which might explain why we were unable to coimmunoprecipitate the 250 and 130 kDa isoforms of PCDH15 or the 120 kDa isoform of CDH23 with any of the Usher proteins tested. Alternatively, it is also possible that as the high molecular weight isoforms of PCDH15 and CDH123 are present at low concentrations, they have been missed in the coimmunoprecipitation experiments.

Of all the Usher proteins that appear in the buoyant fractions of the first sucrose gradient, only harmonin and clarin-1 remain at the top of the gradient after the second sucrose gradient. We were surprised by these results, since harmonin is considered a principal scaffold protein for Usher protein complex formation, and since our coimmunoprecipitation experiments clearly demonstrate interactions between harmonin and other Usher proteins. This is likely due to disruption of the harmonin interactions following addition of nonionic detergent.

It is worth noting that harmonin and clarin-1 are the only Usher proteins expressed all along the full length of the cilia of the tracheal epithelia. This might reflect a distinct function for these two proteins in airway cilia.

The Usher complexes sediment between the 60S and the 40S ribosomal subunits after the second sucrose gradient. Although this is merely an estimation of the size of the complexes, we are able to suggest a molecular mass of approximately 2×10^6 Da for the larger complex and 1.4×10^6 Da for the smaller complex (*60*). It is quite possible that the two complexes may be part of a larger complex that fragmented during the processing and sedimentation procedures. This may explain the disparity between the coimmunoprecipitation data, which shows SANS interacting with the 90 kDa isoform of PCDH15 and the 200 kDa isoform of CDH23, and the sedimentation data, which shows SANS

sedimenting with the smaller complex and CDH23/PCDH15 sedimenting with the larger complex.

In summary, all Usher proteins are expressed in ciliated tracheal epithelial cells, forming large protein complexes highly concentrated in the vesicular subfraction that can be specifically immunoprecipitated with anti-Usher protein antibodies. Disruption of the vesicles in the presence of a chemical chaperone allowed the identification of at least two distinct Usher protein complexes (or fragmented products of a larger complex) with sedimentation coefficients near 40S and 50S containing multiple isoforms of various Usher proteins. Thus, this work provides direct evidence for the existence of large native Usher protein complexes both in vesicles and in the cytosol of tracheal epithelium. Understanding the nature of native Usher protein interactions is a critical step toward unraveling the function of these complexes in hair cells and photoreceptors, which will be important for deciphering the molecular pathobiology of Usher syndrome.

ACKNOWLEDGMENT

The authors gratefully acknowledge Dr. Ulrich Muller for the kind gift of the CDH23(−68) antibody, Skip Kennedy for expert preparation of figures, Dr. Barbara Morley for the use of facilities, and Ms. Jacqueline Pavlik in Dr. Sisson's laboratory for help with the acquisition of the bovine tracheas. We thank Daniel T. Meehan and Duane Delimont for technical support. Confocal microscopy was conducted at the Integrative Biological Imaging Facility at Creighton University, Omaha, NE. This facility was constructed with support from C06 Grant RR17417-01 from the NCRR, NIH.

REFERENCES

1. Hallgren, B. (1959) *Retinitis pigmentosa* combined with congenital deafness; with vestibulo-cerebellar ataxia and neural abnormality in a proportion of cases. *Acta Psychiatr. Scand., Suppl. 138*, 1–100.
2. Nuutila, A. (1970) Dystrophia retinae pigmentosa−dysacusis syndrome (DRD): a study of the Usher or Hallgren syndrome. *J. Genet. Hum. 18* (1), 57–88.
3. Boughman, J. A., Vernon, M., and Shaver, K. A. (1993) Usher syndrome: definition and estimate of prevalence from two high risk populations. *J. Chron. Dis. 36*, 595–603.
4. Ahmed, Z. M., Riazuddin, S., Riazuddin, S., and Wilcox, E. R. (2003) The molecular genetics of Usher syndrome. *Clin. Genet. 63* (6), 431–444.
5. Reiners, J., Nagel-Wolfrum, K., Jürgens, K., Märker, T., and Wolfrum, U. (2006) Molecular basis of human Usher syndrome: deciphering the meshes of the Usher protein network provides insights into the pathomechanisms of the Usher disease. *Exp. Eye Res. 83* (1), 97–119.
6. Weil, D., Blanchard, S., Kaplan, J., Guilford, P., Gibson, F., Walsh, J., Mburu, P., Varela, A., Levilliers, J., and Weston, M. D. (1995) Defective myosin VIIA gene responsible for Usher syndrome type 1B. *Nature 374* (6517), 60–61.
7. Ahmed, Z. M., Riazuddin, S., Bernstein, S. L., Ahmed, Z., Khan, S., Griffith, A. J., Morell, R. J., Friedman, T. B., Riazuddin, S., and Wilcox, E. R. (2001) Mutations of the protocadherin gene PCDH15 cause Usher syndrome type 1F. *Am. J. Hum. Genet. 69* (1), 25–34.
8. Alagramam, K. N., Yuan, H., Kuehn, M. H., Murcia, C. L., Wayne, S., Srisailpathy, C. R., Lowry, R. B., Knaus, R., Van Laer, L., Bernier, F. P., Schwartz, S., Lee, C., Morton, C. C., Mullins, R. F., Ramesh, A., Van Camp, G., Hageman, G. S., Woychik, R. P., and Smith, R. J. (2001) Mutations in the novel protocadherin PCDH15 cause Usher syndrome type 1F. *Hum. Mol. Genet. 10* (16), 1709–1718.
9. Bitner-Glindzicz, M., Lindley, K. J., Rutland, P., Blaydon, D., Smith, V. V., Milla, P. J., Hussain, K., Furth-Lavi, J., Cosgrove, K. E., Shepherd, R. M., Barnes, P. D., O'Brien, R. E., Farndon, P. A., Sowden, J., Liu, X. Z., Scanlan, M. J., Malcolm, S., Dunne, M. J., Aynsley-Green, A., and Glaser, B. (2000) A recessive contiguous gene deletion causing infantile hyperinsulinism, enteropathy and deafness identifies the Usher type 1C gene. *Nat. Genet. 26* (1), 6–7.
10. Verpy, E., Leibovici, M., Zwaenepoel, I., Liu, X. Z., Gal, A., Salem, N., Mansour, A., Blanchard, S., Kobayashi, I., Keats, B. J., Slim, R., and Petit, C. (2000) A defect in harmonin, a PDZ domain-containing protein expressed in the inner ear sensory hair cells, underlies Usher syndrome type 1C. *Nat. Genet. 26* (1), 51–55.
11. Weil, D., El-Amraoui, A., Masmoudi, S., Mustapha, M., Kikkawa, Y., Lainé, S., Delmaghani, S., Adato, A., Nadifi, S., Zina, Z. B., Hamel, C., Gal, A., Ayadi, H., Yonekawa, H., and Petit, C. (2003) Usher syndrome type I G (USH1G) is caused by mutations in the gene encoding SANS, a protein that associates with the USH1C protein, harmonin. *Hum. Mol. Genet. 12* (5), 463–471.
12. Bork, J. M., Peters, L. M., Riazuddin, S., Bernstein, S. L., Ahmed, Z. M., Ness, S. L., Polomeno, R., Ramesh, A., Schloss, M., Srisailpathy, C. R., Wayne, S., Bellman, S., Desmukh, D., Ahmed, Z., Khan, S. N., Kaloustian, V. M., Li, X. C., Lalwani, A., Riazuddin, S., Bitner-Glindzicz, M., Nance, W. E., Liu, X. Z., Wistow, G., Smith, R. J., Griffith, A. J., Wilcox, E. R., Friedman, T. B., and Morell, R. J. (2001) Usher syndrome 1D and nonsyndromic autosomal recessive deafness DFNB12 are caused by allelic mutations of the novel cadherin-like gene CDH23. *Am. J. Hum. Genet. 68* (1), 26–37.
13. Bolz, H., von Brederlow, B., Ramírez, A., Bryda, E. C., Kutsche, K., Nothwang, H. G., Seeliger, M., del C-Salcedó Cabrera, M., Vila, M. C., Molina, O. P., Gal, A., and Kubisch, C. (2001) Mutation of CDH23, encoding a new member of the cadherin gene family, causes Usher syndrome type 1D. *Nat. Genet. 27* (1), 108–112.
14. Sankila, E. M., Pakarinen, L., Kääriäinen, H., Aittomäki, K., Karjalainen, S., Sistonen, P., and de la Chapelle, A. (1995) Assignment of an Usher syndrome type III (USH3) gene to chromosome 3q. *Hum. Mol. Genet. 4* (1), 93–98.
15. Ebermann, I., Scholl, H. P., Charbel Issa, P., Becirovic, E., Lamprecht, J., Jurklies, B., Millán, J. M., Aller, E., Mitter, D., and Bolz, H. (2007) A novel gene for Usher syndrome type 2: mutations in the long isoform of whirlin are associated with retinitis pigmentosa and sensorineural hearing loss. *Hum. Genet. 121* (2), 203–211.
16. Eudy, J. D., Weston, M. D., Yao, S., Hoover, D. M., Rehm, H. L., Ma-Edmonds, M., Yan, D., Ahmad, I., Cheng, J. J., Ayuso, C., Cremers, C., Davenport, S., Moller, C., Talmadge, C. B., Beisel, K. W., Tamayo, M., Morton, C. C., Swaroop, A., Kimberling, W. J., and Sumegi, J. (1998) Mutation of a gene encoding a protein with extracellular matrix motifs in Usher syndrome type IIa. *Science 280* (5370), 1753–1757.
17. van Wijk, E., Pennings, R. J., te Brinke, H., Claassen, A., Yntema, H. G., Hoefsloot, L. H., Cremers, F. P., Cremers, C. W., and Kremer, H. (2004) Identification of 51 novel exons of the Usher syndrome type 2A (USH2A) gene that encode multiple conserved functional domains and that are mutated in patients with Usher syndrome type II. *Am. J. Hum. Genet. 74* (4), 738–744.
18. Petit, C. (2001) Usher syndrome: from genetics to pathogenesis. *Annu. Rev. Genomics Hum. Genet. 2*, 271–297.
19. Kremer, H., van Wijk, E., Märker, T., Wolfrum, U., and Roepman, R. (2006) Usher syndrome: molecular links of pathogenesis, proteins and pathways. *Hum. Mol. Genet. 15* (2), R262–R270.
20. Hasson, T. (1997) Unconventional myosins, the basis for deafness in mouse and man. *Am. J. Hum. Genet. 61* (4), 801–805.
21. Reiners, J., van Wijk, E., Märker, T., Zimmermann, U., Jürgens, K., te Brinke, H., Overlack, N., Roepman, R., Knipper, M., Kremer, H., and Wolfrum, U. (2005) Scaffold protein harmonin (USH1C) provides molecular links between Usher syndrome type 1 and type 2. *Hum. Mol. Genet. 14* (24), 3933–3943.
22. Kalay, E., de Brouwer, A. P., Caylan, R., Nabuurs, S. B., Wollnik, B., Karaguzel, A., Heister, J. G., Erdol, H., Cremers, F. P., Cremers, C. W., Brunner, H. G., and Kremer, H. (2005) A novel D458V mutation in the SANS PDZ binding motif causes atypical Usher syndrome. *J. Mol. Med. 83* (12), 1025–1032.
23. Delprat, B., Michel, V., Goodyear, R., Yamasaki, Y., Michalski, N., El-Amraoui, A., Perfettini, I., Legrain, P., Richardson, G., Hardelin, J. P., and Petit, C. (2005) Myosin XVa and whirlin, two deafness gene products required for hair bundle growth, are located at the stereocilia tips and interact directly. *Hum. Mol. Genet. 14* (3), 401–410.
24. Reiners, J., and Wolfrum, U. (2006) Molecular analysis of the supramolecular Usher protein complex in the retina. Harmonin as the key protein of the Usher syndrome. *Adv. Exp. Med. Biol. 572*, 349–353.
25. van Wijk, E., van der Zwaag, B., Peters, T., Zimmermann, U., Te Brinke, H., Kersten, F. F., Märker, T., Aller, E., Hoefsloot, L. H., Cremers, C. W., Cremers, F. P., Wolfrum, U., Knipper, M., Roepman, R., and Kremer, H. (2006) The DFNB31 gene product whirlin connects to the Usher protein network in the cochlea and retina by direct association with USH2A and VLGR1. *Hum. Mol. Genet. 15* (5), 751–765.
26. Overlack, N., Maerker, T., Latz, M., Nagel-Wolfrum, K., and Wolfrum, U. (2008) SANS (USH1G) expression in developing and mature mammalian retina. *Vision Res. 48* (3), 400–412.

27. Siemens, J., Kazmierczak, P., Reynolds, A., Sticker, M., Littlewood-Evans, A., and Müller, U. (2002) The Usher syndrome proteins cadherin 23 and harmonin form a complex by means of PDZ-domain interactions. *Proc. Natl. Acad. Sci. U.S.A. 99* (23), 14946–14951.
28. Müller, U. (2008) Cadherins and mechanotransduction by hair cells. *Curr. Opin. Cell. Biol. 20* (5), 557–566.
29. Maerker, T., van Wijk, E., Overlack, N., Kersten, F. F., McGee, J., Goldmann, T., Sehn, E., Roepman, R., Walsh, E. J., Kremer, H., and Wolfrum, U. (2008) A novel Usher protein network at the periciliary reloading point between molecular transport machineries in vertebrate photoreceptor cells. *Hum. Mol. Genet. 17* (1), 71–86.
30. Ahmed, Z. M., Riazuddin, S., Aye, S., Ali, R. A., Venselaar, H., Anwar, S., Belyantseva, P. P., Qasim, M., Riazuddin, S., and Friedman, T. B. (2008) Gene structure and mutant alleles of PCDH15: nonsyndromic deafness DFNB23 and type 1 Usher syndrome. *Hum. Genet. 124* (3), 215–223.
31. Pearsall, N., Bhattacharya, G., Wisecarver, J., Adams, J., Cosgrove, D., and Kimberling, W. (2002) Usherin expression is highly conserved in mouse and human tissues. *Hear. Res. 174* (1−2), 55–63.
32. Bhattacharya, G., Miller, C., Kimberling, W. J., Jablonski, M. M., and Cosgrove, D. (2002) Localization and expression of usherin: a novel basement membrane protein defective in people with Usher's syndrome type IIa. *Hear. Res. 163* (1−2), 1–11.
33. Bhattacharya, G., Kalluri, R., Orten, D. J., Kimberling, W. J., and Cosgrove, D. (2004) A domain-specific usherin/collagen IV interaction may be required for stable integration into the basement membrane superstructure. *J. Cell. Sci. 117* (Part 2), 233–242.
34. Bhattacharya, G., and Cosgrove, D. (2005) Evidence for functional importance of usherin/fibronectin interactions in retinal basement membranes. *Biochemistry 44* (34), 11518–11524.
35. McMillan, D. R., Kayes-Wandover, K. M., Richardson, J. A., and White, P. C. (2002) Very large G protein-coupled receptor-1, the largest known cell surface protein, is highly expressed in the developing central nervous system. *J. Biol. Chem. 277* (1), 785–792.
36. Adato, A., Vreugde, S., Joensuu, T., Avidan, N., Hamalainen, R., Belenkiy, O., Olender, T., Bonne-Tamir, B., Ben-Asher, E., Espinos, C., Millán, J. M., Lehesjoki, A. E., Flannery, J. G., Avraham, K. B., Pietrokovski, S., Sankila, E. M., Beckmann, J. S., and Lancet, D. (2002) USH3A transcripts encode clarin-1, a four-transmembrane-domain protein with a possible role in sensory synapses. *Eur. J. Hum. Genet. 10* (6), 339–350.
37. Zallocchi, M., Meehan, D. T., Delimont, D., Askew, C., Garige, S., Gratton, M. A., Rothermund-Franklin, C. A., and Cosgrove, D. (2009) Localization and expression of clarin-1, the Clrn1 gene product, in auditory hair cells and photoreceptors, Hear. Res. (Epub ahead of print).
38. Johnson, K. R., Gagnon, L. H., Webb, L. S., Peters, L. L., Hawes, N. L., Chang, B., and Zheng, Q. Y. (2003) Mouse models of USH1C and DFNB18: phenotypic and molecular analyses of two new spontaneous mutations of the Ush1c gene. *Hum. Mol. Genet. 12* (23), 3075–3086.
39. Siemens, J., Lillo, C., Dumont, R. A., Reynolds, A., Williams, D. S., Gillespie, P. G., and Müller, U. (2004) Cadherin 23 is a component of the tip link in hair-cell stereocilia. *Nature 428* (6986), 950–955.
40. Boëda, B., El-Amraoui, A., Bahloul, A., Goodyear, R., Daviet, L., Blanchard, S., Perfettini, I., Fath, K. R., Shorte, S., Reiners, J., Houdusse, A., Legrain, P., Wolfrum, U., Richardson, G., and Petit, C. (2002) Myosin VIIa, harmonin and cadherin 23, three Usher I gene products that cooperate to shape the sensory hair cell bundle. *EMBO J. 21* (24), 6689–6699.
41. Reiners, J., Reidel, B., El-Amraoui, A., Boëda, B., Huber, I., Petit, C., and Wolfrum, U. (2003) Differential distribution of harmonin isoforms and their possible role in Usher-1 protein complexes in mammalian photoreceptor cells. *Invest. Ophthalmol. Visual Sci. 44* (11), 5006–5015.
42. Reiners, J., Märker, T., Jürgens, K., Reidel, B., and Wolfrum, U. (2005) Photoreceptor expression of the Usher syndrome type 1 protein protocadherin 15 (USH1F) and its interaction with the scaffold protein harmonin (USH1C). *Mol. Vision 11*, 347–355.
43. Lillo, C., Kitamoto, J., and Williams, D. S. (2006) Roles and interactions of Usher 1 proteins in the outer retina. *Adv. Exp. Med. Biol. 572*, 341–348.
44. Adato, A., Lefèvre, G., Delprat, B., Michel, V., Michalski, N., Chardenoux, S., Weil, D., El-Amraoui, A., and Petit, C. (2005) Usherin, the defective protein in Usher syndrome type IIA, is likely to be a component of interstereocilia ankle links in the inner ear sensory cells. *Hum. Mol. Genet. 14* (24), 3921–3932.
45. Adato, A., Michel, V., Kikkawa, Y., Reiners, J., Alagramam, K. N., Weil, D., Yonekawa, H., Wolfrum, U., El-Amraoui, A., and Petit, C. (2005) Interactions in the network of Usher syndrome type 1 proteins. *Hum. Mol. Genet. 14* (3), 347–356.
46. El-Amraoui, A., and Petit, C. (2005) Usher I syndrome: unraveling the mechanisms that underlie the cohesion of the growing hair bundle in inner ear sensory cells. *J. Cell Sci. 118* (Part 20), 4593–4603.
47. Senften, M., Schwander, M., Kazmierczak, P., Lillo, C., Shin, J. B., Hasson, T., Géléoc, G. S., Gillespie, P. G., Williams, D., Holt, J. R., and Müller, U. (2006) Physical and functional interaction between protocadherin 15 and myosin VIIa in mechanosensory hair cells. *J. Neurosci. 26* (7), 2060–2071.
48. Kazmierczak, P., Sakaguchi, H., Tokita, J., Wilson-Kubalek, E. M., Milligan, R. A., Müller, U., and Kachar, B. (2007) Cadherin 23 and protocadherin 15 interact to form tip-link filaments in sensory hair cells. *Nature 449* (7158), 87–91.
49. Wolfrum, U., Liu, X., Schmitt, A., Udovichenko, I. P., and Williams, D. S. (1998) Myosin VIIa as a common component of cilia and microvilli. *Cell. Motil. Cytoskeleton 40* (3), 261–271.
50. Soni, L. E., Warren, C. M., Bucci, C., Orten, D. J., and Hasson, T. (2005) The unconventional myosin-VIIa associates with lysosomes. *Cell. Motil. Cytoskeleton 62* (1), 13–26.
51. McGee, J., Goodyear, R. J., McMillan, D. R., Stauffer, E. A., Holt, J. R., Locke, K. G., Birch, D. G., Legan, P. K., White, P. C., Walsh, E. J., and Richardson, G. P. (2006) The very large G-protein-coupled receptor VLGR1: a component of the ankle link complex required for the normal development of auditory hair bundles. *J. Neurosci. 26* (24), 6543–6553.
52. Deretic, D., and Papermaster, D. S. (1991) Polarized sorting of rhodopsin on post-Golgi membranes in frog retinal photoreceptor cells. *J. Cell. Biol. 113* (6), 1281–1293.
53. Papermaster, D. S., and Dreyer, W. J. (1974) Rhodopsin content in the outer segment membranes of bovine and frog retinal rods. *Biochemistry 13* (11), 2438–2444.
54. Napoli, I., Mercaldo, V., Boyl, P. P., Eleuteri, B., Zalfa, F., De Rubeis, S., Di Marino, D., Mohr, E., Massimi, M., Falconi, M., Witke, W., Costa-Mattioli, M., Sonenberg, N., Achsel, T., and Bagni, C. (2008) The fragile X syndrome protein represses activity-dependent translation through CYFIP1, a new 4E-BP. *Cell 134* (6), 1042–1054.
55. Lagziel, A., Ahmed, Z. M., Schultz, J. M., Morell, R. J., Belyantseva, I. A., and Friedman, T. B. (2005) Spatiotemporal pattern and isoforms of cadherin 23 in wild type and waltzer mice during inner ear hair cell development. *Dev. Biol. 280* (2), 295–306.
56. Tsarouhas, V., Senti, K., Jayaram, S., Tiklova, K., Hemphala, J., Adler, J., and Samakovlis, C. (2007) Sequential pulses of apical epithelial secretion and endocytosis drive airway maturation in *Drosophila*. *Dev. Cell 13*, 214–225.
57. Inden, M., Kitamura, Y., Takeuchi, H., Yanagida, T., Takata, K., Kobayashi, Y., Taniguchi, T., Yoshimoto, K., Kaneko, M., Okuma, Y., Taira, T., Ariga, H., and Shimohama, S. (2007) Neurodegeneration of mouse nigrostriatal dopaminergic system induced by repeated oral administration of rotenone is prevented by 4-phenylbutyrate, a chemical chaperone. *J. Neurochem. 101* (6), 1491–1504.
58. Li, J., Wang, J. J., Yu, Q., Wang, M., and Zhang, S. X. (2009) Endoplasmic reticulum stress is implicated in retinal inflammation and diabetic retinopathy. *FEBS Lett. 583* (9), 1521–1527.
59. Grillet, N., Xiong, W., Reynolds, A., Kazmierczak, P., Sato, T., Lillo, C., Dumont, R. A., Hintermann, E., Sczaniecka, A., Schwander, M., Williams, D., Kachar, B., Gillespie, P. G., and Müller, U. (2009) Harmonin mutations cause mechanotransduction defects in cochlear hair cells. *Neuron 62* (3), 375–387.
60. Nieuwenhuysen, P., and Clauwaert, J. (1981) Physicochemical characterization of ribosomal particles from the eukaryote Artemia. *J. Biol. Chem. 256* (18), 9626–9632.
61. Marriq, C., Rolland, M., and Lissitzky, S. (1977) Polypeptide chains of 19-S thyroglobulin from several mammalian species and of porcine 27-S iodoprotein. *Eur. J. Biochem. 79* (1), 143–149.